

A 2-MeV MICROWAVE THERMIONIC GUN[†]E. Tanabe,[‡] M. Borland,* M. C. Green,[§] R. H. Miller[°] L. V. Nelson[§] J. N. Weaver,* and H. Wiedemann*[‡] AET Associates, Cupertino, CA 95014, USA

* Stanford Synchrotron Radiation Laboratory, Stanford University, Stanford, CA 94309, USA

[§] Varian Associates, Palo Alto, CA 94303, USA[°] Stanford Linear Accelerator Center, Stanford University, Stanford, CA 94309, USA

ABSTRACT

A high-gradient, S-band microwave gun with a thermionic cathode is being developed in a collaborative effort by AET, Varian, and SSRL. A prototype design using an upgraded Varian dispenser cathode mounted with thermal isolation directly in the first half-cell of a 1-1/2 cell, side-coupled, standing-wave cavity has been fabricated and is being tested. Optimization of the cavity shape and beam formation was done using SUPERFISH, MASK, and PARMELA. An overview of design details, as well as the status of in-progress beam tests, will be presented.

INTRODUCTION

In a collaborative effort, AET Associates, Varian Associates (VA) and the Stanford Synchrotron Radiation Laboratory (SSRL) are developing a 2 MeV S-band microwave electron gun. In one application it would be an integral part of a VA medical or radiographic accelerator. In another application it would be part of a SSRL pre-injector for SPEAR as a synchrotron light source. In the first case simplicity and compactness are the design criteria. The goal is to be able to mount a cathode directly in the first half cell of a standard VA side-coupled, standing-wave accelerator section. Thus, the normally-used 20 kV gun insulator and pulse-transformer winding would be eliminated, but cathode thermal isolation and back-bombardment heating problems might be substituted. In the second case, a 1-1/2 cell (plus one side-coupling cell) microwave gun will generate a train of bunches that will be compressed in time by an alpha magnet and narrowed in energy spread by slits built into the alpha magnet. A fast, FET-switched chopper-collimator at the entrance to a 150 MeV linac will allow selection of three bunches out of the several thousand that are produced over a range of energies and during several microwave gun cavity fill times.

Some of the earliest experiments with microwave guns probably were with a hot tungsten filament inserted in the first cell of a Hansen Laboratory disk-loaded, traveling-wave accelerator section. Significant current control and energy spread problems were undoubtedly encountered. More recent efforts at Hansen Laboratory^{1,2} involved a separate gun with a lanthanum hexaboride cathode in a RF cavity, followed by an alpha magnet. Currently, there is considerable interest by some research groups to employ laser-pulsed photocathodes,^{3,4} hot and cold. With such cathodes, control of the current and pulse length is inherently easy, but the system cost and complexity is greatly increased.

DESIGN AND TESTS

This section discusses a design and tests that are in progress with a prototype microwave gun. Figure 1 shows a cross-sectional view of this high-gradient 1-1/2 cell, S-band gun. A demountable cathode structure was designed so that an RF choke joint around the cathode stem can be installed if necessary, and various cathode materials can be tested in the future. The initial design incorporates an alumina thermal barrier around the cathode stem. This barrier has been metallized and

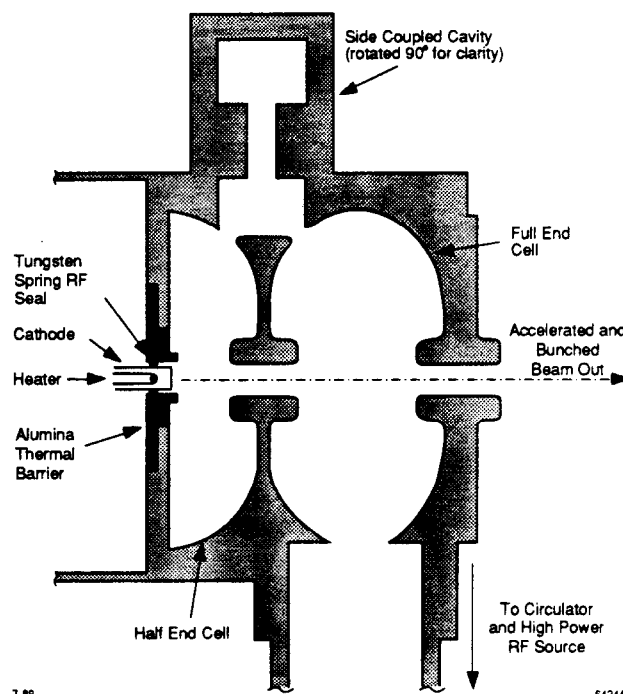


Fig. 1: Cross-sectional view of the 1-1/2 on-axis cells.

copper-plated (~ 0.01 mm). RF contact between the stem and the barrier is made via a tungsten-wire spring in the form of a toroid to further decrease conductive heat losses from the cathode. An annular-focus electrode protrudes into the half-cell RF fields from the thermal barrier surrounding the cathode. The electrode shape was determined using MASK⁵ to obtain proper focusing, while maintaining a high shunt impedance and a high accelerating field, E_p , on axis. The gun is over-coupled through an iris in the full cell to a standard S-band rectangular waveguide. For a maximum beam-loading power of 3 MW, which corresponds to an average beam energy of 2 MeV at 1.5 A, the RF power lost in the cavity walls would be approximately 1 MW. If $\beta \approx 4$ with no beam, the cavity will appear to be matched when beam-loaded, as in this example.

The RF gun employs a high-performance, impregnated-tungsten dispenser cathode that is coated with a Varian-developed, emission-enhancing layer in order to lower the effective work-function of the activated cathode material. This layer is comprised of a sputtered coating of an osmium alloy that is crystallographically oriented to preferentially expose a single-crystal plane at the emitting surface. The layer microstructure is controlled so that the individual crystallites are columnar and are no more than 1000-2000 Å in lateral extent. This results in a very narrow spread in the work-function across the cathode surface, and permits fully space-charge-limited operation at current densities of over 100 A/cm² with moderate temperatures in order to achieve high intrinsic brightness. Cathodes of this type⁶ with diameters up to 5.1 cm have been made at VA and tested with current densities of up to 140 A/cm².

[†]Work supported in part by the United States of America Department of Energy, Office of Basic Energy Sciences, Division of Chemical/Material Sciences, Department of Energy contract DE-AC03-76SF00515, and by Varian Associates, Radiation Division.

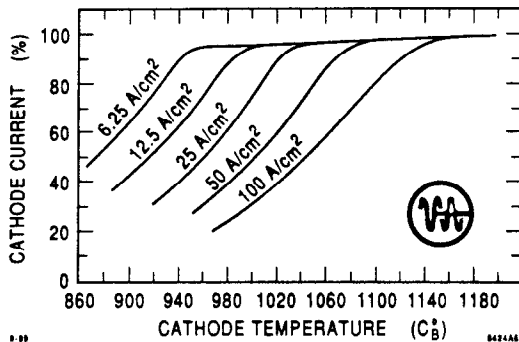


Fig. 2: Cathode current versus temperature for a Varian 100 A/cm² dispenser cathode.

Measured brightnesses exceeding 1×10^{10} A/(m-rad)² have been recorded. Figure 2 shows a typical, experimentally-determined, temperature-limited curve for such a cathode.

In the half-cell containing the cathode, there is a cut-off aperture on the wall opposite to the side-coupling cell aperture that is designed to serve both as a vacuum pumpout port and as a symmetrical RF perturbation, in order to minimize field distortion along the beam centerline in the vicinity of the cathode, where the beam is least stiff. Two 8 l/s vacuum ion pumps were installed, one directly on the first half-cell and the other on the input rectangular waveguide.

Since the microwave gun current will be controlled by varying the cathode temperature in a way similar to that prescribed in Fig. 2, a feedback circuit on the heater power supply will be necessary to stabilize this current. The problem is exacerbated by cathode heating from back-bombardment, which is especially characteristic of RF guns. Cavity frequency tuning will be accomplished thermally, and it may include feedback to control the cooling water temperature. Tests of the thermal characteristics of the cavity are in progress. Subsequently, RF power will be applied and the beam characteristics will be measured.

The design goals that were established for the gun, for operation as part of the SSRL pre-injector are: (1) for a current density at the cathode of $J \leq 100$ A/cm², each bunch injected into the linac should contain at least 10^9 usable electrons; i.e., electrons with momenta $\geq 80\%$ of the peak momentum in the bunch, (2) manageable back-bombardment power; i.e., less than 5 W average, (3) 2 to 3 MeV/c peak momenta in the bunches, (4) linear, monotonic dependence of momentum, $p(t)$, on time for 20 to 40 ps during a bunch in order to allow bunch compression by an alpha magnet, (5) well-controlled, transverse beam-size over a wide range of cathode current densities (10 A/cm² < J < 100 A/cm²) for field levels that produce 2 to 3 MeV/c peak momentum and (6) rms geometric (unnormalized) emittance of less than 3π mm mrad in both planes, over the same range of conditions.

COMPUTER SIMULATIONS

In this section, various simulations of the gun are discussed with regards to which parameters were varied in order to optimize the design, and what is the predicted performance of the final design. The primary tool for simulating the gun was the program MASK, which is a fully relativistic and electromagnetic particle-in-cell code. The program is very CPU-intensive and is typically run on a super-computer. For present purposes, MASK was modified to run on SSRL's VAX 8810 computer. MASK results were tested partially with a program called RFGUN⁷ which integrates the longitudinal equations of motion in the presence of the electric field profiles calculated by SUPERFISH⁸ and in

the absence of space charge. Calculations with the simpler and less-accurate program PARMELA gave similar results to those given by MASK.

Ideally, one would simulate the entire gun, including the coupling cell, for a full RF pulse, which could be as long as $2 \mu\text{s}$. or 5700 RF periods for 2856 MHz. The cathode would emit particles throughout the simulation, although at first these particles would not exit even the first cell. With such a simulation, one could verify that, at some point in the operating cycle, useful electron bunches would emerge from the gun. One could also demonstrate whether or not, in the presence of beam, the cavity oscillated as desired in the π -mode, with the required field ratio between the two cells. Since beam-loading power is expected to exceed wall losses by as much as a factor of 3, it is possible that the equilibrium field configuration reached by the gun with beam will be different from that reached with no beam. Unfortunately, a single such simulation would take roughly six years of CPU time!

Rather than simulate the entire operating cycle of the gun, it was decided to assume that the gun would reach equilibrium with the desired field configuration, in which case it is only necessary to simulate a single RF cycle with beam. From such a simulation, the beam-loading power at the assumed equilibrium can be calculated and used to assess the input power needed by the gun. The fundamental mode of the cells can be excited very efficiently by an antenna driven for four RF periods by a shaped, sinusoidal pulse. With proper pulse shaping and proper placement of the antenna, excitation of other modes can be kept below 10^{-3} of the fundamental. Emission of particles from the cathode can be started on the fifth RF cycle, and the complete simulation need only run for seven cycles.

The first and second cells of the gun were simulated separately, in part to obviate the need to simulate the coupling cell, and in part to allow easier independent variation of the electric field strength in the two cells. The boundary conditions between the two cells cannot be properly simulated in this way, but this proved unimportant since the particles of interest have kinetic energies of over 200 keV by the time they reach the interface. Small frequency differences between the two cells are inevitable due to the nonzero mesh size of the simulations. These are compensated for by adjusting the relative phases to be slightly different from π . Thus, when electrons arrive in the second cell, the field configuration is very close to that which would exist if the cells oscillated at the same frequency and with a phase difference of π .

Having made the decision to design a gun based on a 1-1/2 cell side-coupled standing-wave cavity, the most convenient parameter at our disposal for modifying the longitudinal distribution was the ratio of the on-axis, peak electric fields, E_{p1} , in the two cells. For the i^{th} cell, where $i = 1, 2$, the electric fields on-axis have the form $E_{zi}(z, t) = E_{pi} E_{ni}(z) \sin(\omega t + \phi_i)$, where the $E_{ni}(z)$ are the mode patterns, normalized to unity. The relative excitation of the two cells is thus characterized by $\alpha \equiv E_{p2}/E_{p1}$.

In order to keep back-bombardment power low, α was made appreciably greater than unity, which means that the particles will gain most of their energy in the second cell. In order to avoid break-down problems, E_{p2} was kept below 80 MV/m, which corresponds to a peak surface field of about 160 MV/m. It was found from simulations with RFGUN that for $2 < \alpha < 3$ and 50 MV/m < E_{p2} < 80 MV/m, design criteria (3) and (4) could be met. If E_{p2} is kept constant, then a larger α has the advantage of reducing the back-bombardment power and producing high energies without increasing the nonlinearities in $p(t)$. A smaller α results in more charge entering the second cell, but in greater back-bombardment power on the cathode.

A value of $\alpha \approx 3$ was obtained for the prototype gun. For this α , 40-60% of the particles emitted from the cathode reach the second cell, depending on E_{p2} . The vast majority of the

particles that do not reach the second cavity return to hit the cathode, but with about half the average kinetic energy of the particles that exit the first cell. For $60 \text{ MV/m} < E_{p2} < 80 \text{ MV/m}$, 85–90% of the particles in the second cell exit by the desired route. The remaining particles are accelerated back into the first cell or hit the cavity walls.

The transverse distribution is affected by many factors, including the rate of acceleration in the first cell, the focusing nose near the cathode, the size of the cathode, the current density, the radial electric fields produced by the noses in the second cell, and the thermal energy of electrons (this latter effect is negligible). Of these, the focusing nose near the cathode, the size of the cathode, and the current density are most readily varied and controlled. The rate of acceleration in the first cell is limited by the desire to keep back-bombardment low. For simplicity in construction and design, the noses in the second cell were unaltered from a standard Varian design. However, due to the RF nature of the focusing from these noses, they affect the beam emittance, and modifying their shape may be worthwhile in future designs.

To the authors' knowledge, there is no prescription for optimum radial fields near the cathode for an RF gun that emits a long pulse, for which the time dependence of the RF focusing dominates the emittance, though such a criterion does exist for a short pulse.^{3,9} From simulations with MASK, it was found that the emittance is a weak function of the shape and position of the focusing noses, provided that the beam is not focused to a waist in the first cell. Hence, the focusing was made only weakly convergent; i.e., only sufficient to keep the beam from hitting the "anode" nose and the drift-tube walls between the first and second cells. In order to further reduce transverse space-charge effects and maximize the lifetime of the cathode, the cathode current density was kept low by using a 6-mm-diameter cathode. A beam tube diameter of 7.6 mm was chosen to maintain a high shunt impedance with minimum beam interception. No claim is made that the optimum possible combination has been found.

Figure 3 shows the comparison of numerical results from SUPERFISH and experimental results from a bead-drop

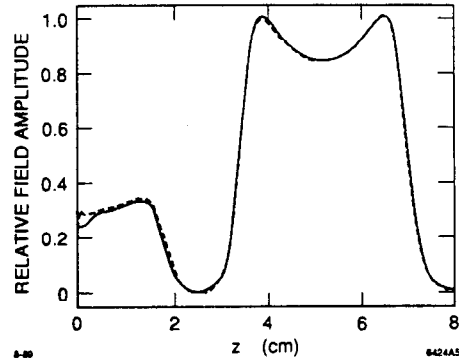


Fig. 3: The longitudinal electric field profile along the beam centerline through the gun (solid = computed; dashed = measured).

measurement of the axial electric field of the cavity of Fig. 1. Figures 4(a), (b) and (c) shows that the beam size increases as the current density is increased for a fixed accelerating field. A comparison of Figs. 4(a) and (d) shows that the beam size—and, in fact, the emittance—decreases with decreased accelerating field; for the lower accelerating field, this smaller emittance may be a result of less charge entering the second cell. Figure 5 gives the energy spectra versus bunched-beam charge, Q , for various RF accelerating field levels. Figure 6 shows the dependence of emittance and accelerated charge on the peak cathode current.

ACKNOWLEDGMENTS

The authors wish to thank R. Tol, who machined the RF cavity, and W. Leong and S. Skellenger, who helped to conduct the tests and experiments. The advice and support of T. I. Smith of HEPL and L. M. Young of LANL was appreciated in using the generic accelerator program PARMELA.

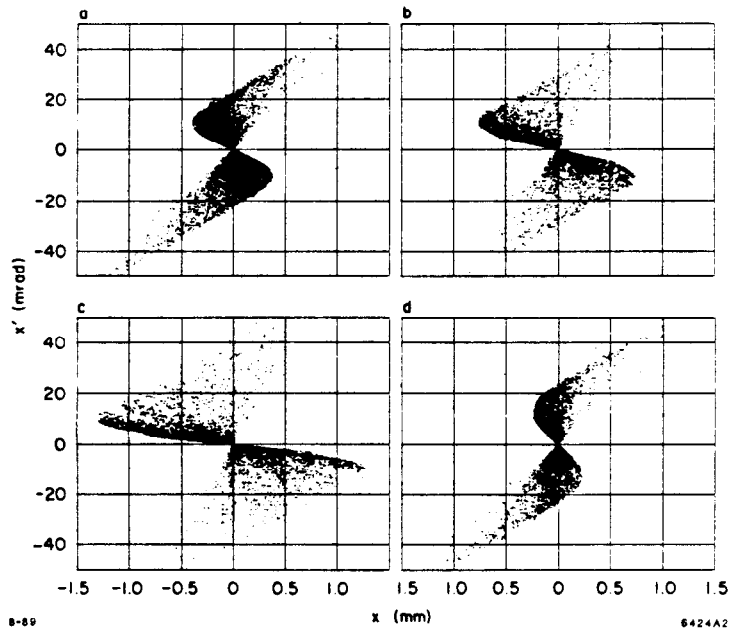


Fig. 4: Transverse phase-space distribution at the gun exit with $\alpha = 3$ in all cases: (a) $E_{p2} = 75 \text{ MV/m}$ and $J = 10 \text{ A/cm}^2$, (b) $E_{p2} = 75 \text{ MV/m}$ and $J = 40 \text{ A/cm}^2$, (c) $E_{p2} = 75 \text{ MV/m}$ and $J = 80 \text{ A/cm}^2$, and (d) $E_{p2} = 60 \text{ MV/m}$ and $J = 10 \text{ A/cm}^2$.

REFERENCES

1. G. A. Westenskow and J. M. J. Madey, *Laser and Particle Beams*, Vol. 2, Part 2 (1984) 223-5.
2. G. A. Westenskow *et al.*, "Owner's Manual for the Microwave Electron Gun," HEPL TN-86-1, Hansen Laboratory, Stanford University, Stanford, CA 94309 (February 1986), unpublished.
3. K. T. McDonald, "Design of the Laser-Driven RF Electron Gun for the BNL Accelerator Test Facility," *IEEE Trans. ED-35* (November 1988), 2052-9.
4. J. S. Fraser and R. L. Sheffield, "High-Brightness Injectors for RF-Driven Free Electron Lasers," *IEEE J. of Quantum Electron. QE-23* (September 1987), 1489-96.
5. A. T. Drobot *et al.*, "Numerical Simulation of High Power Microwave Sources," *IEEE Trans. NS-32* (October 1985), 2733-7.
6. W. C. Turner *et al.*, "High-Brightness, High-Current-Density Cathode for Induction Linac FELs," 1988 Linear Accelerator Conf., Williamsburg, VA, October 3-7, 1988.
7. M. Borland, "RFGUN—A Program for Simulating RF Guns," SSRL ACD NOTE 78.
8. K. Halbach and R. F. Holsinger, "SUPERFISH—A Computer Program for Evaluation of RF Cavities with Cylindrical Symmetry," *Particle Accelerators* 7 (1976), 213-22.
9. M. E. Jones and W. K. Peter, *Proc. 6th Int. Conf. on High-Power Particle Beams*, Kobe, Japan (June 1986); LANL doc. LA-UR-86-1941.

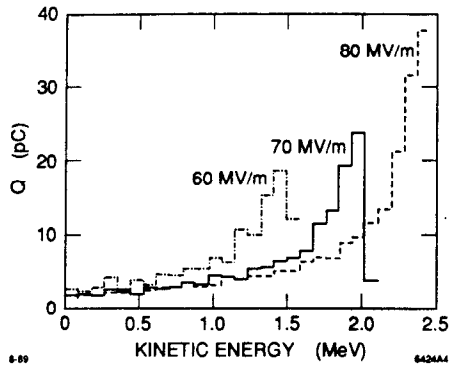


Fig. 5: Energy spectra at gun exit for several values of E_{p2} with the cathode surface current density held at $J = 10 \text{ A/cm}^2$.

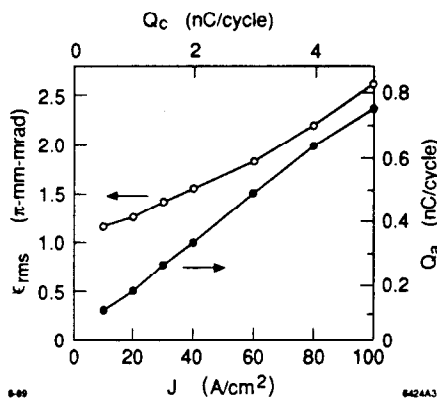


Fig. 6: MASK results for the geometric (unnormalized) beam emittance. $\epsilon_{rms} \equiv (\sigma_x^2 \sigma_x^2 - \sigma_{xx}^2)^{1/2}$, and "useful" accelerated charge per bunch, Q_a , as a function of the charge emitted from the cathode surface, Q_c , or the surface current density, J , for $E_p = 75 \text{ MV/m}$, $\alpha = 3$ and $\gamma \geq 4.4$ (or $E \geq 1.74 \text{ MeV}$).